35th Annual International Conference of the IEEE EMBS
Osaka, Japan, 3 - 7 July, 2013

SOURCE LOCALIZATION TECHNIQUES FOR DIRECTION DECODING FROM LOCAL FIELD POTENTIALS

Vijay Aditya Tadipatri[†] *Ahmed H. Tewfik*[†] *James Ashe*[⋆] *Guiseppe Pellizzer*[⋆]

[†]The University of Texas at Austin, Austin, TX, USA [⋆] University of Minnesota, Twin Cities, MN, USA

ABSTRACT

Local Field Potential (LFP) recordings are one type of intracortical recordings, (besides Single Unit Activity) that can help decode movement direction successfully. In the long-term however, using LFPs for decoding presents some major challenges like inherent instability and non-stationarity. Our approach to overcome this challenge bases around the hypothesis that each task has a signature source-location pattern. The methodology involves introduction of source localization, and tracking of sources over a period of time that enables us to decode movement direction in an eight-direction center-out-reach-task. We establish that such tracking can be used for long term decoding, with preliminary results indicating consistent patterns. In fact, tracking task related source locations render up to 66% accuracy in decoding movement direction one week after the decoding model was learnt.

Index Terms— Sparse Source Localization, Local Field Potentials, Movement Decoding.

I. INTRODUCTION

One of the main problems with using single unit activity or local field potentials for long term task decoding is their inherent instability and non-stationarity [1]. Only a fraction of the recorded sites remains stable over two weeks [2], making it difficult to obtain long term decoding. Since most of the pattern recognition techniques developed to decode the behavioral tasks depend on the consistency and stability of observed data, they fail to provide good long term decoding. Also, most reported literature uses cross-validation to evaluate algorithms, providing an optimistic estimate of the achievable decoding [3], [4]. While studies show the reliable intracortical recordings over hundreds of days, daily retraining is needed to obtain consistent decoding [5].

Our hypothesis is that behavioral tasks are defined by certain consistent and stable underlying patterns. In this paper, we propose that these patterns are defined by sources that generate local field potentials. We provide evidence that by tracking their trajectories over trial time, arm movement decoding can be achieved. During this study, we observe that the source locations and their trajectories remain consistent over time and thus enable the decoding of these tasks without the need of retraining.

In the past, several techniques like Minimum Norm Solution, Weighted Minimum Norm Solution, Low resolution brain tomography analysis (LORETA) and standardized-LORETA (s-LORETA) [6], [7], have been proposed to estimate the source locations for neural signal recording modalities like EEG, MEG, and ECoG data. In these techniques, the solution is obtained by solving a linear system of dipole lead-field projections of all possible locations of dipoles on a given sensor arrangement. The drawback of these techniques is that they provide solutions that spread the energy over all source locations, as there are more source locations than the total number of sensors for the observed signal. This makes the system under-determined and leads to an infinite number of solutions. To obtain a more meaningful solution we constrain the problem to a sparse space, under the assumption that only a few active sources are active at any time instant; solutions to which can be obtained with algorithms like LASSO, Focal Underdetermined System Solver (FOCUSS) etc.[8]. Most of the methods enforce sparse formulation on the three dipole moment coordinates and this tends to bias the dipole location towards a certain moment coordinate componenet. Hence, we use a solution that is invariant to the rotations of dipole moments but the total dipole moment is constrained [9], [10]. While these methods constrain the overall dipole distribution to be sparse, the dipole moment at certain locations can reach values that are physiologically infeasible. In our formulation, we specifically ensure that dipole moment at all locations is under a physiological bound. By focussing only on the location of these estimated dipoles at successive time-instants we can overcome the instability due to the variation of dynamic range over multiple days. In this paper, we show that this strategy is successful to decode movement direction over two weeks after the model training is performed.

The paper is organized in the following way: Section II describes the neural signal acquisition and behavioral tasks performed by the monkey subjects; Section III discusses the algorithm for sparse source estimation and the decoding algorithm to decode the neural data; Section IV presents the preliminary results that were obtained using the proposed algorithm and a comparison with the state-of-the-art methods; Section V provides concluding remarks and some suggested future work.

978-1-4577-0216-7/13/$26.00

II. DATA

Two male rhesus monkeys (H464, H564) were trained to perform the center-out-target-reach task with a robotic manipulandum. The subjects were implanted in the primary and dorsal premotor areas with two 64-grid Utah microelectrode arrays. Each array was arranged on a 10×10 grid of width 4mm with equal separation between the electrodes. The experimental paradigm and the preprocessing are the same as in [11]. For monkey H464, the sessions were performed over a two week period with the following chronology: session 1 on day 1, sessions 2 and 3 a week from session 1 and sessions 4 and 5 two weeks from session 1. For the monkey H564, only three such sessions were performed before it progressed to another experiment. All the trials in a particular session were presented to the subject in a randomized order. Figure 1 shows the pseudo-random time spent by the subject at each cue of a single trial. At the successful completion of such a trial subjects were given a juice reward and only these trials were included in the analysis. The number of successful trials depended on the motivation of the monkey, varying from 10 per direction in the least successful session to 35 per direction in the most successful one. During the preprocessing stage, time-frequency analysis and histograms were used to remove channels that had low Signal to Noise Ratio (SNR) or high baseline wander, thus retaining 61 channels for H464 and 98 for H564. The next section discusses the algorithm used for decoding movement directions.

III. ALGORITHM

The hypothesis of our approach is that each neural task has certain underlying sources. First, we discuss the algorithm to perform the sparse source localization from the observed neural recordings.

III-A. Source Localization

We begin the source localization algorithm description with the classical framework used for source estimation.

$$y = Ax \tag{1}$$

where $y \in \mathbb{R}^M$ is signal observed on M sensors at a single time instant, $x \in \mathbb{R}^{3N}$ is a vector of dipole intensities at N potential dipole locations, with dipole moments in 3 dimensions and $A \in \mathbb{R}^{M \times 3N}$ is the lead-field matrix for the sources. We choose the dipole source model as it provides

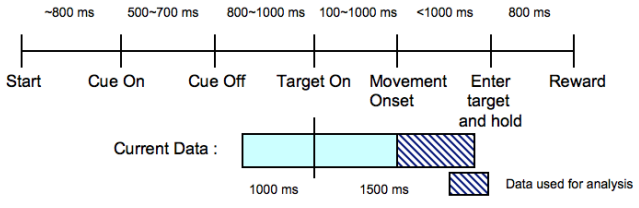

Fig. 1: Time-line of the neural data to be used in the analysis.

an easily interpretable model. In general, $N >> M$, making the linear system under-constrained and thus has an infinite solution space. Since it is assumed that only a few of the sources are active at any given time, they can be identified by adding a sparsity constraint. The $l0$ norm is a non-convex constraint and the $l1$ norm is chosen as a closer approximation to enforce sparsity.

The solution for these equations can be formulated as follows:

$$\widehat{x} \quad = \quad \min \|y - Ax\|_2 + \lambda \|x\|_1 \tag{2}$$

where λ is a regularization parameter to incorporate sparsity with the l_1-norm constraint. Please note that $x = [\rho_x^1, \rho_y^1, \rho_z^1, ..., \rho_x^N, \rho_y^N, \rho_z^N]$, where ρ represents the dipole moment in each of the 3 dimensions. The above formulation provides a solution by enforcing the constraint on all the moment dimensions. To provide a constraint that is invariant to the rotations in these dimensions, we use a slightly modified version as shown below [10].

$$\widehat{x} \quad = \quad \min \|y - Ax\|_2 + \lambda \|\rho\|_1, \tag{3}$$

where $\rho \in \mathbb{R}^N$ is the absolute moment at a given location, defined as

$$\rho(n) = \sqrt{\rho_x^{n\mathbf{2}} + \rho_y^{n\mathbf{2}} + \rho_z^{n\mathbf{2}}} \tag{4}$$

Since gradient based methods cannot be directly applied to the problem in 3, as it is not differentiable at zero, we convert it into a reduced second-order cone programming (SOCP) problem:

$$\begin{aligned} \{\widehat{x}, \widehat{q}, \widehat{z}\} \quad &= \quad \min q + \lambda z, \\ \text{s.t. } \|y - Ax\|_2 \leq q, \quad & \sum \rho(n) \leq z \\ \forall \rho(n) < \rho_{max} & \end{aligned} \tag{5}$$

where λ is the regularization parameter that addresses the balance between the number of dipoles used in the solution and the reconstruction error. The parameters q and z are introduced to convert the problem into a linear problem with second-order cone constraints. ρ_{max} is a physiological bound on the dipole moments at all locations. Equation (5) is a convex problem and can be solved efficiently using the primal-dual interior-point method implemented by the Self Dual Minimization software (SeDuMi) [12].

III-B. Decoding

As mentioned in section II, each task involves the movement of arm over time and neural signal is acquired over multiple time instants. Consider $\mathbf{Y} = [y_1 y_2 ... y_T] \in \mathbb{R}^{M \times T}$, be the neural recordings observed at T time samples of the behavioral task. Once the dipole location for each time instant is estimated, we retain the dipole the location and intensity as a feature. The value of λ is chosen to provide the best decoding in the training trials in terms of the area under the receiver operator curve (AUC).

We identified spatial and temporal locations that provide the best discrimination. For example, figure 3 shows the area

under the curve (for classification of 0°and 90°) at different spatial locations over 1s of trial time after the movement onset. Only the features that have area under the curve more than 0.9 are retained and used for classification. A linear support vector machine (SVM) is trained on these features to obtain the decoding model. We used multiple and redundant binary classifiers in error correction output codes (ECOC) framework [11]. In such a framework, all possible 1-vs-1 classifiers are trained, along with hierarchical classifiers where neighboring directions are pooled into a super class. For every new trial that needs to be decoded, sparse source locations are estimated using the same procedure and the SVM model is used to decode movement of the trial, based on these features.

IV. RESULTS

In our analysis, we have neural measurements from the primary motor and the premotor grid areas with the aid of two planar sensor arrangements as mentioned in section II. We use the dipole forward model to calculate the lead-field matrix for each of the two grids separately and assume that the dipoles closer to the primary motor area do not influence the sensors on the premotor area and vice-versa. When an arrangement with multiple planeswas tested, the solutions lied only on the plane closest to the sensor grid. Hence, only the dipoles located on the same plane, parallel to the sensor grid arrangement are estimated. Based on such a formulation the lead-field matrix for both the grids can be written as

$$A = \begin{bmatrix} A_{pri} & \mathbf{0} \\ \mathbf{0} & A_{pre} \end{bmatrix} \tag{6}$$

where A_{pri} and A_{pre} are the lead-field matrices for the primary motor area and premotor area respectively.

The spatial resolution of the dipole location is chosen to be half the inter-electrode distance. This resolution of the sources can be increased at the expense of processing time. However, we observed only slight improvement when the resolution was further increased. We chose the value of λ that provided the minimum cross-validation error on the training session. We also observed that certain spatial locations have active dipoles up to the onset of movement and these locations become inactive once the movement begins. This behavior is especially observed in dipoles from the premotor area, which remain predominantly inactive during movement but are active before the movement onset and also after the target is reached. An example of such a behavior is shown in Figure 2. Another interesting observation is that the maximum decoding (high AUC) occurs right after the movement is onset as can be inferred from Figure 3.

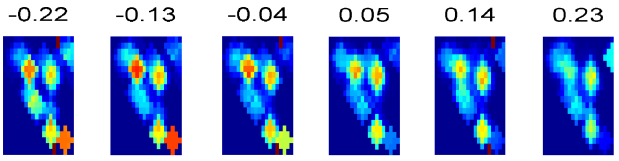

Fig. 2: The behavior of certain dipoles before movement onset. Each sub figure represents the dipole grid near the primary motor area at the time instant. The color of the figure is scaled such that deep red indicates high number of trials that had an active dipole in a particular location at that instant and deep blue indicates no active dipoles. As seen in this figure, the dipoles in the bottom right of the grid are active in most of the trials, only up to the movement onset (0s) and are inactive after that.

Table I: Comparison of Decoding Powers across various algorithms for H464 and H564. The decoding models are trained on the 1^{st} day and tested on sessions conducted after about a week and two.

H464				
Day after Training	8	9	13	14
CSP [13]	38%	41%	16%	13%
Rank CSP [11]	62%	60%	48%	39%
Dipole Tracking	66%	61%	44%	42%
H564				
Day after Training	8	9		
CSP [13]	41%	40%		
Rank CSP [11]	51%	49%		
Dipole Tracking	50%	42%		

To evaluate our algorithm we trained the model on the trials only from session on day 1. For this purpose, the recordings were filtered in the δ-band (0-4Hz) and 1s of data after the movement onset is analysed as shown in Figure 1. The models were trained on data collected on day 1 and their performance was evaluated on data collected in the future sessions. The measure used for comparison is the decoding power (or decoding accuracy) and is defined as the ratio of number of correctly predicted trials to the total number of trials. The decoding performance from source estimation is compared with results from state-of-the-art techniques like common spatial patterns (CSP) and its variants. To maintain consistency and have a good comparison, we use the same ECOC classifiers for CSP and source decoding techniques. For classification by chance, the decoding power is 12.5% for a set of eight targets.

Table I compares the decoding power of the suggested method with those obtained by CSP [13]. From the table we can infer that the model provided by estimating the dipole locations provides better decoding. The CSP algorithm overfits the training data as it relies on the raw neural recording and does not consider the effects of non-stationarity, instability and learning that modulate and alter the neural patterns from day-to-day. By considering only the spatial locations and the trajectories of the active dipoles for each task, the proposed method overcomes the changes in dynamic range similar to the Rank CSP [11]. Thus, it is able to obtain comparable decoding powers over a two week time-line.

V. CONCLUSION

In this paper, we have provided a new formulation to decode the movement directions based on the estimates of the dipole source locations. Specifically, we show that each of the neural task is performed by sequential dipole activations in a certain pattern. These patterns are unique to the movement task and can be used to reliably decode movement directions. Further, these patterns are very stable and based on this hypothesis, we provide evidence that

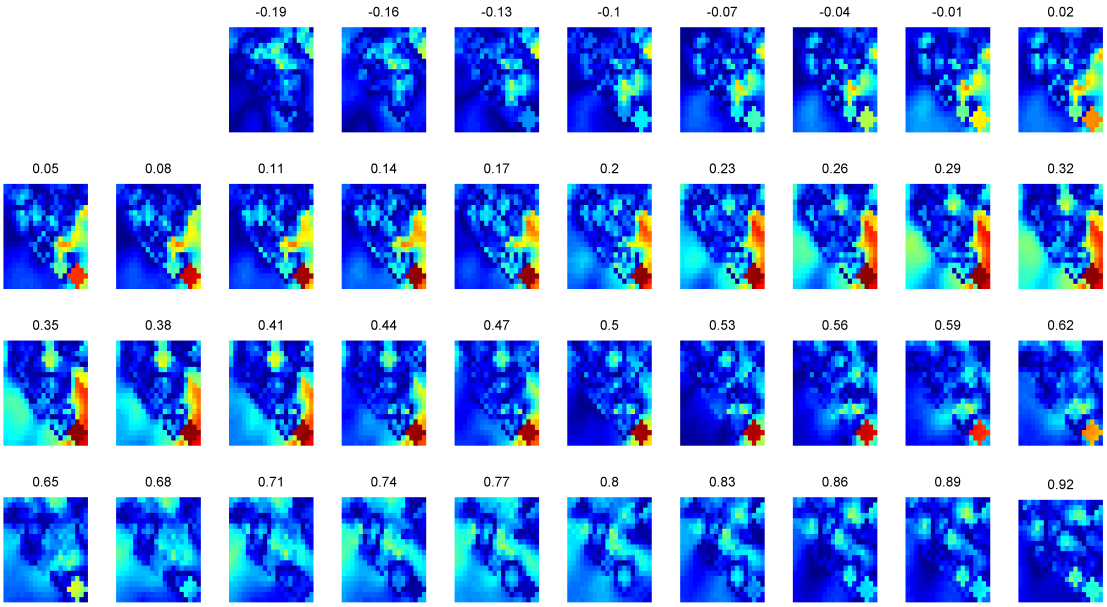

Fig. 3: The discrimination ability, in terms of AUC between movements to targets at 0°and 90°, of the spatial and temporal dipole intensities for monkey H464 in session 1. Each sub figure represents the dipole grid near the primary motor area at the time instant indicated above it. These are aligned such that the movement onset is at 0ms. The color of the figure is scaled - deep red indicates high degree of discriminationand deep blue no discrimination.

tracking such source locations can decode 8 movement directions with an accuracy of up to 66% in subsequent sessions. These preliminary results are encouraging and further improvements can be pursued. One such improvement is to obtain a solution that is temporally smooth, rather than a separate solution for each time instant as suggested here.

The tracking of dipole activations can also throw light on the effects of learning and the changes in neural patterns over a long time. Further analysis is needed in understanding the changes in the dipole activation patterns when a new task is introduced to the subject. Also, while the focus of the analysis in this paper has been on movement onset epoch, a similar analysis can be extended to epochs of target planning before the actual movements.

VI. REFERENCES

[1] Winnie Jensen and Patrick J. Rousche, "On variability and use of rat primary motor cortex responses in behavioral task discrimination," *Journal of Neural Engineering*, vol. 3, no. 1, pp. L7+, Mar. 2006.

[2] Adam S. Dickey, Aaron Suminski, Yali Amit, and Nicholas G. Hatsopoulos, "Single-Unit Stability Using Chronically Implanted Multielectrode Arrays," *Journal of Neurophysiology*, vol. 102, no. 2, pp. 1331–1339, Aug. 2009.

[3] Carsten Mehring, Jörn Rickert, Eilon Vaadia, Simone Cardosa de Oliveira, Ad Aertsen, and Stefan Rotter, "Inference of hand movements from local field potentials in monkey motor cortex.," *Nature neuroscience*, vol. 6, no. 12, pp. 1253–1254, Dec. 2003.

[4] John G. O'Leary and Nicholas G. Hatsopoulos, "Early Visuomotor Representations Revealed From Evoked Local Field Potentials in Motor and Premotor Cortical Areas," *J Neurophysiol*, vol. 96, no. 3, pp. 1492–1506, Sept. 2006.

[5] J D Simeral, S-P Kim, M J Black, J P Donoghue, and L R Hochberg, "Neural control of cursor trajectory and click by a human with tetraplegia 1000 days after implant of an intracortical microelectrode array," *Journal of Neural Engineering*, vol. 8, no. 2, pp. 025027, 2011.

[6] Roberta Grech, Tracey Cassar, Joseph Muscat, Kenneth P Camilleri, Simon G Fabri, Michalis Zervakis, Petros Xanthopoulos, Vangelis Sakkalis, and Bart Vanrumste, "Review on solving the inverse problem in EEG source analysis," *Journal of neuroengineering and rehabilitation*, vol. 5, pp. 25, 2008, PMID: 18990257.

[7] Roberto D. Pascual-Marqui, "Discrete, 3D distributed, linear imaging methods of electric neuronal activity. part 1: exact, zero error localization," *arXiv:0710.3341*, Oct. 2007.

[8] I F Gorodnitsky, J S George, and B D Rao, "Neuromagnetic source imaging with FOCUSS: a recursive weighted minimum norm algorithm," *Electroencephalography and clinical neurophysiology*, vol. 95, no. 4, pp. 231–251, Oct. 1995, PMID: 8529554.

[9] Lei Ding and Bin He, "Sparse source imaging in electroencephalography with accurate field modeling," *Human Brain Mapping*, vol. 29, no. 9, pp. 1053–1067, 2008.

[10] Wanmei Ou, Matti S. Hämäläinen, and Polina Golland, "A distributed spatio-temporal EEG/MEG inverse solver," *NeuroImage*, vol. 44, no. 3, pp. 932–946, Feb. 2009.

[11] Vijay Aditya Tadipatri, Ahmed H. Tewfik, Vikrham B. Gowreesunker, J. Ashe, G. Pellizer, and R. Gupta, "Time robust movement direction decoding in local field potentials using channel ranking," in *Engineering in Medicine and Biology Magazine*. IEEE, 2010, vol. 29.

[12] Jos F. Sturm, *Using SeDuMi 1.02, a MATLAB toolbox for optimization over symmetric cones*, 1998.

[13] Benjamin Blankertz, Motoaki Kawanabe Ryota Tomioka, Friederike U. Hohlefeld, Vadim Nikulin, and Klaus-robert Müller, "Invariant common spatial patterns: Alleviating nonstationarities in brain-computer interfacing," in *In Ad. in NIPS 20*, 2008, vol. 20.